Int J Thermophys (2009) 30:1423–1437
DOI 10.1007/s10765-009-0626-y

Thermal Damage Analysis in Biological Tissues Under Optical Irradiation: Application to the Skin

Félix Fanjul-Vélez · Noé Ortega-Quijano · José Ramón Solana-Quirós · José Luis Arce-Diego

Received: 14 October 2008 / Accepted: 13 July 2009 / Published online: 29 July 2009

Abstract The use of optical sources in medical praxis is increasing nowadays. In this study, different approaches using thermo-optical principles that allow us to predict thermal damage in irradiated tissues are analyzed. Optical propagation is studied by means of the radiation transport theory (RTT) equation, solved via a Monte Carlo analysis. Data obtained are included in a bio-heat equation, solved via a numerical finite difference approach. Optothermal properties are considered for the model to be accurate and reliable. Thermal distribution is calculated as a function of optical source parameters, mainly optical irradiance, wavelength and exposition time. Two thermal damage models, the cumulative equivalent minutes (CEM) 43 °C approach and the Arrhenius analysis, are used. The former is appropriate when dealing with dosimetry considerations at constant temperature. The latter is adequate to predict thermal damage with arbitrary temperature time dependence. Both models are applied and compared for the particular application of skin thermotherapy irradiation.

Keywords Arrhenius analysis · Bio-heat equation · CEM 43 °C approach · Optical treatment · Thermal damage · Thermo-optical properties

F. Fanjul-Vélez (✉) · N. Ortega-Quijano · J. L. Arce-Diego
Applied Optical Techniques Group, ETSII y de Telecomunicación,
TEISA Department, University of Cantabria, Av. de los Castros S/N,
39005 Santander, Spain
e-mail: fanjulf@unican.es

J. R. Solana-Quirós
Thermodynamics and Statistical Physics Group, Applied Physics Department,
University of Cantabria, Av. de los Castros S/N, 39005 Santander, Spain

1 Introduction

The application of engineering to medicine is revolutionizing medical praxis. For instance, tools like endoscopes or ultrasound imaging allow practitioners to see tissues in a way they could have never imagined. Among these technological advances, optical methods become more important nowadays, both in treatment and characterization of biological tissues. The application of optics to the field of medicine is a promising tool for the development of new methods of treatment of disorders and of tissue observation with greater detail and contrast, for example, by means of optical coherence tomography (OCT) [1] or fluorescence spectroscopy [2]. Besides characterization applications, optical techniques provide also new treatment possibilities, and the appropriate study of their effects uses thermo-optical principles. Two examples of optical treatment by optical irradiation are photodynamic therapy (PDT) [2] and low intensity laser therapy (LILT) [2]. LILT relies on the administration of low intensity optical radiation as a therapeutic procedure, where sometimes the application of subsequent different light exposures improves the final result. PDT uses optical radiation to stimulate the reaction of a substance inoculated previously to the patient. This compound usually provokes tissue necrosis, so it is normally used in tumor elimination. Another very interesting implementation is thermotherapy, which consists of controlling temperature increase in a pathological biological tissue. With this method it is possible to provoke an improvement on specific diseases, but a previous analysis of treatment is needed in order for the patient not to suffer any collateral damage, an essential point due to security margins in medical procedures. If the temperature increase is aimed at tissue necrosis, like in cancer, it is called hyperthermia [3].

In this study, we analyze different approaches that allow us to predict thermal damage in tissues irradiated by optical sources. These models require temperature distribution data. The next section presents the optical propagation model considered, which uses the radiation transport theory (RTT) equation, solved via a Monte Carlo analysis. In Sect. 3 a thermal model, taking into account conduction, convection, radiation, blood perfusion, and vaporization depending on the specific problem, is explained in detail. The spatial–temporal differential bio-heat equation is solved via a numerical finite difference approach. Thermal distribution is calculated as a function of optical source parameters, mainly optical irradiance, wavelength, and exposition time. These data are used as inputs in thermal damage models. Section 4 describes the two thermal damage models we consider, the cumulative equivalent minutes (CEM) 43 °C approach and the Arrhenius analysis. In Sect. 5 both models are applied and compared for the particular application of skin thermotherapy irradiation. Optothermal skin properties are provided for the model to be accurate and reliable. The most appropriate is proposed as a predictive thermal damage tool in specific optical treatments.

2 Optical Model of Light Propagation in Tissue

There are several approaches to model light propagation in tissue [2]. As is known, the fact that biological tissues are heterogeneous media makes this task even more

complex, because analytical solutions are only available for simple geometries, such as spheres or cylinders [4]. As a consequence, an abstraction consisting of substituting the real tissue for an ideal material in which spheres of another material are randomly located is usually assumed. With this model, the effects that are taken into account are reflection, absorption, and scattering, and therefore the parameters that describe light propagation in tissue are the index of refraction n (dimensionless), the absorption coefficient $\mu_a(\mathrm{m}^{-1})$ and the scattering coefficient $\mu_s(\mathrm{m}^{-1})$. In this kind of problem, the most difficult effect to model is scattering, because its appropriate study has to do with different approaches related to the ratio between light wavelength and particle size, in the so-called geometric, Rayleigh and Mie analyses [5].

Many models work with the assumption made previously, such as Kubelka–Munk [2], that uses a two flux approximation, a seven flux approach [6], or even an exponential approach in a one-dimensional problem [7]. As was stated in the introduction, here a three-dimensional model, based on the radiation transport theory (RTT), will be used. This model assumes that scattering events are sufficiently numerous, and so light can be considered incoherent, in such a way that polarization or interference effects can be neglected. In this way, the basic parameter of light is the specific intensity, $I\left(\vec{r},\hat{s},t\right)\left(\mathrm{W}\cdot\mathrm{m}^{-2}\cdot\mathrm{sr}^{-1}\right)$, that is, the light power per unit area per unit solid angle. The radiation is expected to be at point $\vec{r}$, and to follow the $\hat{s}$ direction. Scattering events are treated according to the scattering phase function, $p\left(\hat{s},\hat{s}'\right)$, which contains the probability of light to be scattered in the different directions. Light comes from direction $\hat{s}'$ and is redirected to $\hat{s}$. The basic mechanism in order to express the temporal differential radiation transport equation is that radiation interacting with a particle attenuates due to absorption and scattering and also gains power because other particles can scatter light in the direction of interest. This idea is expressed in Eq. 1, which is one of the fundamental laws of this thermo-optical model [2]:

$$\frac{1}{c_m\frac{\mathrm{d}}{\mathrm{d}t}}I\left(\vec{r}(t),\hat{s},t\right)=-\left(\mu_a+\mu_s\right)I\left(\vec{r}\,(t),\hat{s},t\right)+\frac{\mu_s}{4\pi}\int p\left(\hat{s},\hat{s}'\right)I\left(\vec{r}(t'),\hat{s}',t\right)\mathrm{d}\Omega'+Q\left(\vec{r}(t),\hat{s},t\right),\quad(1)$$

where c_m is the speed of light in the medium, Ω refers to the solid angle, and $Q\left(\vec{r}\,(t),\hat{s},t\right)$ represents a source placed at the point of interest. For our purposes, there are no sources inside the tissue and a steady-state situation can be considered. In this case, $\frac{\mathrm{d}}{\mathrm{d}t}I\left(\vec{r}(t),\hat{s},t\right)=0$ and $Q\left(\vec{r}(t),\hat{s},t\right)=0$. With this assumption in mind, we can rewrite the equation in this way:

$$\hat{s}\cdot\bar{\nabla}I(\vec{r},\hat{s})=-\left(\mu_a+\mu_s\right)I(\vec{r},\hat{s})+\frac{\mu_s}{4\pi}\int_{4\pi}p\left(\hat{s}\cdot\hat{s}'\right)I\left(\vec{r},\hat{s}'\right)\mathrm{d}\Omega'.\quad(2)$$

Although this equation could be solved in an analytical way, the problem is usually simplified by considering approaches in some limiting cases, such as the absorption-dominant limit or diffusion approximation, depending on the relative importance of absorption and scattering events in a particular biological tissue. Apart from that, as

in any problem governed by a differential equation, there is another possibility to solve it: using a numerical approximation. There are several numerical methods, like the finite element or the discrete-ordinates approaches [8]. In this specific topic of the radiation transport equation, the Monte Carlo method is considered a very good approximation to the real problem. The random character of the process makes such an iterative method appropriate.

The Monte Carlo numerical method can use various implementations. One of the most used Monte Carlo methods applied to the RTT model was developed by Wang and Jacques [9]. They programmed the Monte Carlo method in standard C. The key point is the inclusion of the random character on a computer, by means of a mathematical probability analysis, in such a way that numbers with any probability distribution can be obtained from numbers that follow a uniform distribution between 0 and 1. Light is treated as a sequence of photons, whose number is intended to be representative of the accuracy of the solution obtained. One photon is launched and its trajectory, affected by scattering, and absorption are calculated, while the energy at each point is stored. Cylindrical symmetry is assumed, because laser beams usually show this kind of behavior, so in fact the data can be interpreted as coming from a 3-D analysis. The complete tissue is divided in a two-dimensional grid in the r and z directions. As usual, more accurate results require a smaller grid, but the need of a reduced time of computation imposes a trade-off.

The program is used to calculate several parameters. From the point of view of this study concerning thermotherapy, the most important one is the absorption of each element of the grid, due to the fact that it will be the seed of the thermal model. The fluence rate is also shown along with the reflectance and transmittance as a function of the radial position and the angle of observation. This implementation of the Monte Carlo model is also multi-layered, so it is possible to define several layers of different materials, with their borders always perpendicular to the laser beam, which is very useful due to the fact that tissues usually can be divided in different strata. For the appropriate definition of the model, the characteristics and dimensions of each layer are required. The optical parameters needed are the index of refraction, n, the absorption coefficient, μ_a, the scattering coefficient, μ_s, and the anisotropy of scattering, g. This last parameter is also called the average cosine of scatter (dimensionless), and it is related to the scattering phase function by the following relationship [2]:

$$g = \frac{\int\limits_{4\pi} p\left(\hat{s}\cdot\hat{s}'\right)\hat{s}\cdot\hat{s}'\mathrm{d}\Omega'}{\int\limits_{4\pi} p\left(\hat{s}\cdot\hat{s}'\right)\mathrm{d}\Omega'} = \frac{1}{4\pi W_o}\int\limits_{4\pi} p\left(\hat{s}\cdot\hat{s}'\right)\hat{s}\cdot\hat{s}'\mathrm{d}\Omega' = \frac{1}{2W_o}\int\limits_{4\pi} p\left(\cos\theta\right)\cos\theta\sin\theta\mathrm{d}\theta, \tag{3}$$

where the so-called albedo is defined by

$$W_o = \frac{1}{4\pi}\int\limits_{4\pi} p\left(\hat{s}\cdot\hat{s}'\right)\mathrm{d}\Omega' = \frac{\sigma_s}{\sigma_a+\sigma_s} = \frac{\mu_s}{\mu_a+\mu_s}. \tag{4}$$

In this equation, σ_a and σ_s stand for the scattering and absorption cross section, and represent the ratio of the scattered and absorbed optical power to the incident power, respectively. The average cosine of scatter gives an idea about the probability of being scattered in a particular direction. For instance, $g = 0$ implies that all directions are equally probable. If $g > 0$, the radiation tends to be scattered forward, and vice versa. The albedo simply shows the predominance of absorption or scattering in a particular tissue.

The key point in order to achieve a good model of the tissue under interest is the possession of all the optical parameters of the different layers in which the tissue is divided [2,10]. It is clear that, as we are dealing with a simplified model of reality, the lack of accuracy in these parameters will increase greatly the error probability.

3 Thermal Model of Radiated Tissue

In the previous section the optical distribution of light in a biological tissue was calculated. With these data, and taking into account the thermal properties of the sample, our objective now is the achievement of a model that gives us temperature maps associated with that radiation. The model used will consider the influence of spatial and temporal coordinates, so time-dependent analysis will be developed. Afterwards, thermal damage will be estimated from temperature distributions.

The study of the thermal effects in a material involves a knowledge of the main mechanisms of heat transmission [11]. Conduction stands for the diffusion of heat in a solid from hot regions to colder ones, convection involves the interaction between a solid surface and a fluid in contact with it, and radiation refers to the heat transport due to the infrared emission of a body at a nonzero temperature. The application of these considerations about heat transmission to biological tissues follows the general theory with the exception of some particularities. The point now is to obtain a differential equation that allows us to represent the spatial–temporal temperature distribution in a tissue, which is called a bio-heat equation. As usual, there are several approaches to this objective, for instance those developed by Pennes, by Chen, and Holmes, the Weinbaum, Jiji, and Lemons (WJL) model, or the Wissler model [12].

The process for obtaining a bio-heat equation will be described. As was stated above, the main idea is the achievement of a spatial–temporal thermal model. The process starts with the definition of a balance equation that models thermal energy in the tissue:

$$Q_{\text{gain}} = Q_{\text{storage}} + Q_{\text{loss}} + W. \tag{5}$$

Each element admits an integral expression. The heat gained depends on the volumetric heat generated $q(\vec{r}, t)$ in the $\vec{r}$ position and time t, and the heat storage is related to the temperature increase and the thermal parameters of the particular tissue:

$$Q_{\text{gain}} = \int_V q(\vec{r}, t)\, \mathrm{d}V \tag{6}$$

$$Q_{\text{storage}} = \int_V \rho c \frac{\mathrm{d}T\,(\vec{r},t)}{\mathrm{d}t}\mathrm{d}V, \tag{7}$$

where the temperature is represented by T (in K), tissue density is ρ (in $\mathrm{kg{\cdot}m^{-3}}$), and the specific heat is c (in $\mathrm{J\cdot kg^{-1}\cdot K^{-1}}$). The term W in Eq. 5 can be neglected here because it represents the heat internally generated. Thermal losses are compounded, on one hand, by the effect of conduction in the tissue, which is expressed as an area (S) integral,

$$Q_{\text{cond}} = -\int_S k\nabla T\,(\vec{r},t)\,\hat{n}\mathrm{d}S, \tag{8}$$

where the parameter k is the thermal conductivity (in $\mathrm{W\cdot m^{-1}\cdot K^{-1}}$) and vector $\hat{n}$ represents the normal to the surface through which conduction is considered. On the other hand, biological tissues suffer from blood perfusion, that is, the significant effect of blood flow in in vivo treatment of tissue. There are some models that deal with this specific problem [12]. In this case, the one proposed by Pennes is used. The basic parameters by means of which the model is defined are the volumetric perfusion w_{b} (in $\mathrm{m^3_{blood}\cdot s^{-1}\cdot kg^{-1}_{tissue}}$), and the venous and arterial temperatures:

$$Q_{\text{perfusion}} = -\rho_{\mathrm{b}} c_{\mathrm{b}} w_{\mathrm{b}}\,(T_{\text{art}} - T_{\text{ven}}) \tag{9}$$

The subscript b stands for blood, and the absence of a subscript stands for tissue. With Eqs. 6–9 the bio-heat equation can be expressed as [11]

$$\int_V q\,(\vec{r},t)\,\mathrm{d}V = \int_V \rho c \frac{\mathrm{d}T\,(\vec{r},t)}{\mathrm{d}t}\mathrm{d}V - \int_S k\nabla T\,(\vec{r},t)\,\hat{n}\mathrm{d}S - \int_V \rho_{\mathrm{b}} c_{\mathrm{b}} w_{\mathrm{b}}\left[T_{\text{art}}\,(\vec{r},t) - T_{\text{ven}}\,(\vec{r},t)\right]\mathrm{d}V. \tag{10}$$

In the same way as the RTT equation for optical propagation in tissue, Eq. 10 can be solved analytically or numerically, and here again a numerical method is used due to the complexity of the analytical solution. Numerical approximations are mainly the finite difference method and the finite element method [13]. An explicit finite difference method, which transforms the differential equation to a difference equation that can be solved in an iterative way, is chosen [14]. The derivatives are substituted by means of the Taylor expansion, and appropriate boundary conditions must be defined for each element of the established grid which is not situated inside the tissue.

As cylindrical symmetry was assumed in the previous analysis of optical propagation in tissue, the same assumption will be taken in the thermal model, so a two-dimensional grid is defined to solve a real three-dimensional problem. Thermal properties are considered constant in each layer, and the temporal evolution can be followed. The heat generated by the laser source is represented by $q\,(\vec{r},t)$ in Eq. 10.

There is another important fact when dealing with this bio-heat equation, the definition of the boundary conditions. They will strongly depend on the geometrical configuration of the problem considered. As we have in general a 2-D grid, representing depth and radius of a rotating solid, there will be problems in principle in its four boundaries. The left boundary is usually solved because cylindrical symmetry implies that the temperature at the other side of the depth axis must not change, what is expressed mathematically as $\frac{dT}{dr} = 0$. Right and bottom boundaries are normally continuations also of the tissue, and if the grid is sufficiently large so as to cover almost all the significantly heated area, equivalent zero gradients can be assumed, $\frac{dT}{dr} = 0$ and $\frac{dT}{dz} = 0$. The most interesting boundary is usually the upper one, because as radiation comes from that side, it is the part in contact with the environment. Depending on the specific case we are dealing with, effects like convection or radiation should be taken into account [11]. The usual condition of a biological tissue irradiated from the outside, that considers convection by the external fluid (air in most cases) and heat radiation, can be expressed as

$$-k\frac{dT}{dz} = h_c\,(T_e - T_s) + \sigma\varepsilon\left(T_e^4 - T_s^4\right) + h_{fg}h_m\,(\rho_e - \rho_{sat}), \tag{11}$$

where h_c is the convection coefficient (in $W \cdot m^{-2} \cdot K^{-1}$), T_e is the environmental temperature in the external medium, T_s is the temperature of the tissue surface, $\sigma = 5.69610^{-8}\ W \cdot m^{-2} \cdot K^{-4}$ is the Stefan–Boltzmann constant, ε is the emissivity or ratio of the surface radiation to that of an ideal blackbody (dimensionless), h_{fg} is the phase-change enthalpy of water (in $W \cdot s \cdot kg^{-1}$) at T_s, h_m is the convection mass transfer coefficient (in $m \cdot s^{-1}$), ρ_e is the density of water vapor in air, and ρ_{sat} is the density of saturated water vapor at T_s.

Next Figs. 1 and 2 show some results of applying an explicit finite difference numerical method to the differential bio-heat equation, with the boundary conditions previously exposed, on skin. Skin opto-thermal parameters are summarized in Table 1. The fact that they come from a spatial–temporal bio-heat equation makes the influence of exposition duration fundamental. In this way, graphs represent the irradiation by means of a solid-state AlInGaP diode laser that emits at 633 nm, with a power of 0.2 W and 0.8 W. Figure 1 represents the temperature increase distribution after 10 s of irradiation with a 5 mm beam radius. It can be appreciated that an increase of more than 20 K is achieved. In Fig. 2, radiation power is decreased to 0.2 W, and exposition time is increased to 1 min and 20 s. In this case, the maximum temperature increase is reduced (below 20 K), but the heat distribution is more spread.

4 Thermal Damage Models in Tissue

Temperature maps can be obtained from the thermo-optical model previously described. These data allow a good prediction of the adequateness of the optical source parameters for the intended thermotherapy treatment. However, it would be extremely interesting to be able to calculate an estimation of the possible thermal damage the

Table 1 Thermo-optical properties of skin

From top to bottom	Layer	d (mm)	μ_a (cm^{-1})	μ_s (cm^{-1})	g	n	ρ ($g \cdot cm^{-3}$)	c ($J \cdot g^{-1} \cdot K^{-1}$)	$k \times 10^3$ ($W \cdot cm^{-1} \cdot K^{-1}$)	$w_b \times 10^7$ ($cm^3_{blood} \cdot s^{-1} \cdot g^{-1}_{tissue}$)
1	Epidermis	0.06	25	480	0.79	1.5	1	3.77	2.09	0
2	Upper dermis	0.56	2.7	187	0.82	1.4	1	3.77	3.075	7.51
3	Blood plexus	0.1	25	400	0.98	1.35	1	3.77	3.075	7.51
4	Lower dermis	0.56	2.7	187	0.82	1.4	1	3.77	3.075	7.51
5	Subcutaneous fat	0.32	0.2	20	0.8	1.45	0.85	1.96	2.09	35.07
6	Muscle	>2	11.2	530	0.94	1.37	1.05	3.94	6.42	4.509

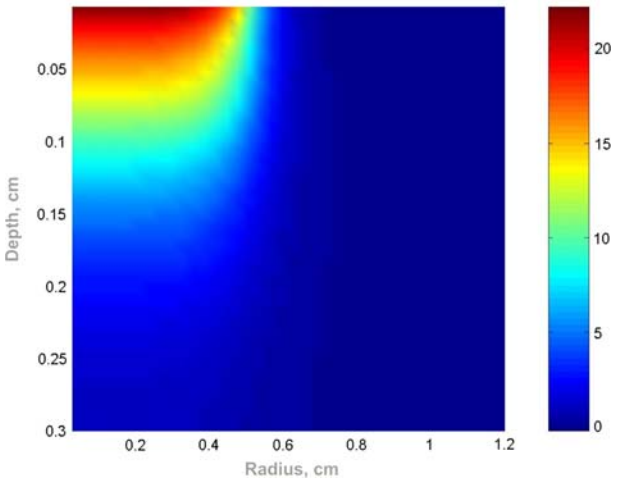

Fig. 1 Temperature increase (K) in skin after 10 s irradiation by a 633 nm source and 1.02 $W \cdot cm^{-2}$

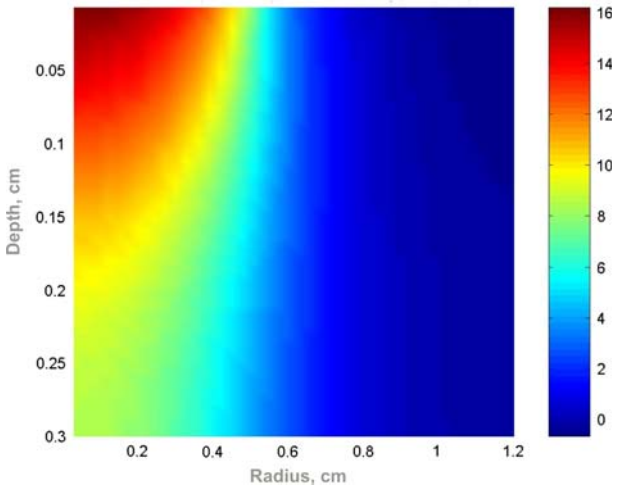

Fig. 2 Temperature increase (K) in skin after 1 min and 20 s irradiation by a 633 nm source and 0.25 $W \cdot cm^{-2}$

application of laser could provoke. There are some approaches to solve this problem, like CEM 43 °C dosimetry [3] or the Arrhenius integral [15]. In this section both of them will be described.

CEM 43 °C dosimetry is appropriate for topics related with safe temperature ranges in tissue, because it is more orientated to the achievement of thermal damage at a constant temperature. CEM stands for cumulative equivalent minutes at 43 °C. These equivalent minutes are calculated by means of the following formula:

$$\mathrm{CEM} = t M^{(43-T)} \tag{12}$$

In this expression, t is the time interval at temperature T (°C). M is the number of minutes needed to compensate 1 °C of temperature change. This value is usually dependent on the specific temperature of the tissue. In case there are several temperatures involved in the time interval considered, it would be necessary to calculate the equivalent minutes at each constant temperature range. Afterwards, all the minutes should be added.

The Arrhenius model takes into account temperature distributions that vary with time. This method is based on the so-called Arrhenius integral:

$$\Omega(\tau) = \ln\left(\frac{C(0)}{C(\tau)}\right) = \int_0^{\tau} A\mathrm{e}^{\left(-\frac{E_\mathrm{a}}{RT}\right)}\mathrm{d}t, \tag{13}$$

where $\Omega(\tau)$ is the thermal damage, A is the frequency factor (in s^{-1}), E_a is the activation energy of the process (in $\mathrm{J}\cdot\mathrm{mol}^{-1}$), R is the universal gas constant (8.32 $\mathrm{J}\cdot\mathrm{mol}^{-1}\cdot\mathrm{K}^{-1}$), $C(0)$ is the percentage of living cells at the beginning of irradiation, and $C(\tau)$ is the same percentage at the end of the treatment after an exposition of τ seconds. Basic parameters are A and E_a, which depend on the specific tissue we are dealing with and control the speed of cellular necrosis. The thermal damage value is directly related with the concentration of alive and dead cells. The exponential nature of Eq. 12 makes the process start with almost no effect on tissue, and after some time, thermal damage increases rapidly.

From this fundamental Eq. 12, some additional useful parameters can be obtained. For instance, it is possible to calculate the speed of change of thermal damage, as its first derivative:

$$\frac{\mathrm{d}(\Omega(\tau))}{\mathrm{d}t} = A\mathrm{e}^{\left(-\frac{E_\mathrm{a}}{RT}\right)} \tag{14}$$

Another important value for the study of thermal damage is the temperature that makes thermal damage rate equal to 1, something called critical temperature (T_crit):

$$T_\mathrm{crit} = \frac{E_\mathrm{a}}{R\ln(A)} \tag{15}$$

The importance of the critical temperature is related to the thermal damage parameters, frequency factor A, and activation energy E_a. When trying to obtain them for the specific tissue we are studying, we must take into account that critical temperatures of its main compounds could be known, so a relationship between both of them can be established. This makes thermal damage analysis easier.

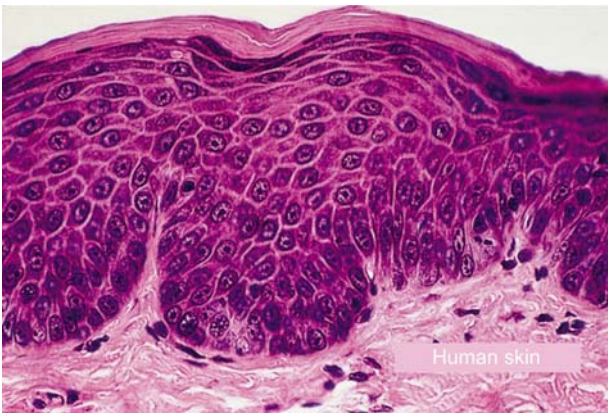

Fig. 3 Histology of healthy skin

Table 2 Thermal damage parameters for CEM 43°C and Arrhenius models on skin

CEM 43 °C		Arrhenius	
M		Activation energy (kcal · mol^{-1})	
<47 °C	>47 °C	(44–47) °C	(47–60) °C
0.13	0.72	182.2	95.78

5 Application of Thermal Models to the Skin

Once we describe the thermal damage models we consider in this article, we will compare them when applied to the skin. This tissue is chosen based on the great applicability of optical treatment techniques, due to the fact that it is easily accessible.

As we saw in previous sections, first a thermo-optical model of skin must be constructed to apply thermal damage models. Histology coming from Marqués de Valdecilla University Hospital shows a skin layer structure (Fig. 3), and optical and thermal properties can be measured. Table 1 shows the thermo-optical properties of skin used in our model. Temperature distributions obtained are used as a seed for thermal damage models. A diagram of the model is shown in Fig. 4.

The application of thermal models needs some specific parameters. In the case of the CEM 43 °C model, the value of M is required, and for Arrhenius analysis, we need the activation energy. These parameters are obtained usually experimentally, and are showed in Table 2.

In order to compare both models, we make a calculation that consists of representing thermal damage at three constant temperatures as time increases. In the case of the Arrhenius integral, the results show thermal damage and in the case of CEM 43 °C, the data correspond to equivalent minutes. Figures 5 and 6 show the results.

In Figs. 5 and 6 there are some arrows that facilitate the comparison. In Fig. 5 it can be appreciated that thermal damage at 43 °C during 60 s is near 2. To obtain the same damage value at 44 °C and 45 °C, exposition times of 24 s and 10 s are needed.

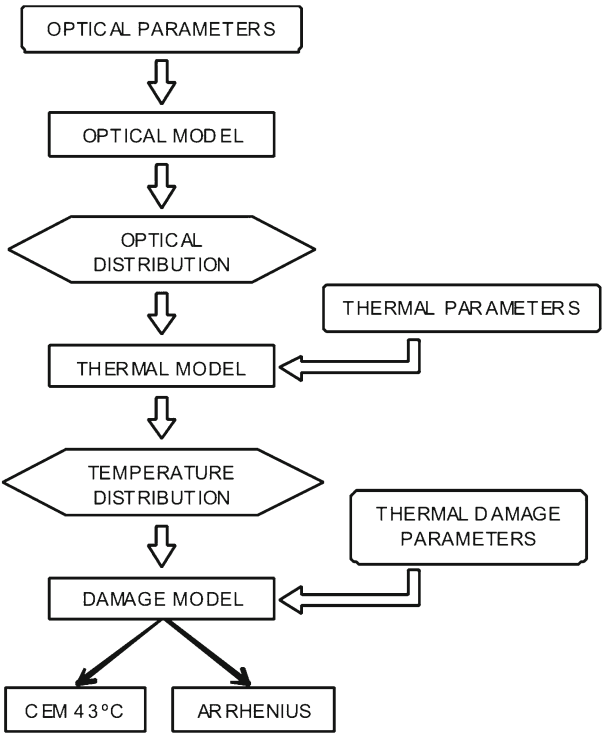

Fig. 4 Diagram of the opto-thermal and damage model

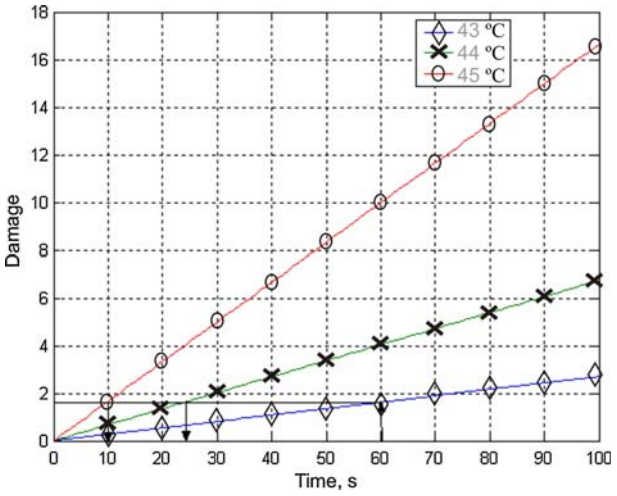

Fig. 5 Thermal damage results with Arrhenius integral

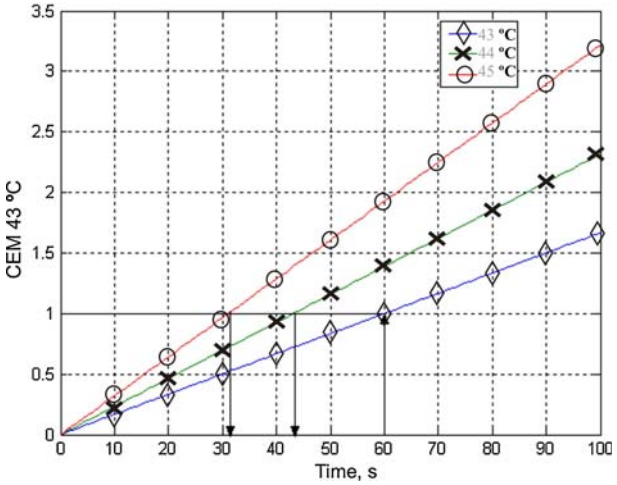

Fig. 6 Thermal damage results with CEM 43 °C

Results of Fig. 6 show that after 60 s at 43 °C, the equivalent minutes at 43 °C are 1, as was expected. However, to obtain the same equivalent minutes at 44 °C and 45 °C, tissue should be exposed for 43 s and 32 s according to this model. By means of these graphs, it can be easily seen that the results of both models are quite different. These differences are mainly due to the inaccuracy of parameter values and also to the procedures of both approaches themselves. Furthermore, the CEM 43 °C model is more appropriate for constant temperature expositions, and it does not provide an absolute damage value, but just a comparison with the situation at 43 °C. On the contrary, the Arrhenius analysis provides absolute thermal damage values and can easily take into account temperature changes during the time interval of interest. As a consequence, the Arrhenius model is preferable for practical applications.

Figure 7 shows the results of the application of the Arrhenius model to laryngeal skin tissue. A laser of 532 nm with 100 mW and 1 W power is employed, and different exposition times are considered. As was expected, the maximum thermal damage is located at the laser impact point, represented in the graphs in the upper left corner. This worst case thermal damage is translated to the survival cell rate by means of Eq. 13. The laser irradiation procedure provokes a non-constant temporal temperature pattern, which is assumed by the Arrhenius model. When irradiating with 100 mW during some seconds, the survival cell rate is high (at least 94 % in the worst case). However, if power is incremented to 1 W, after an exposition of only 2 s, the survival rate is only 1 %. That means that the tissue is almost completely destroyed. A change in any of these various laser parameters would allow us to predict thermal damage in the specific thermotherapy application with which we are dealing.

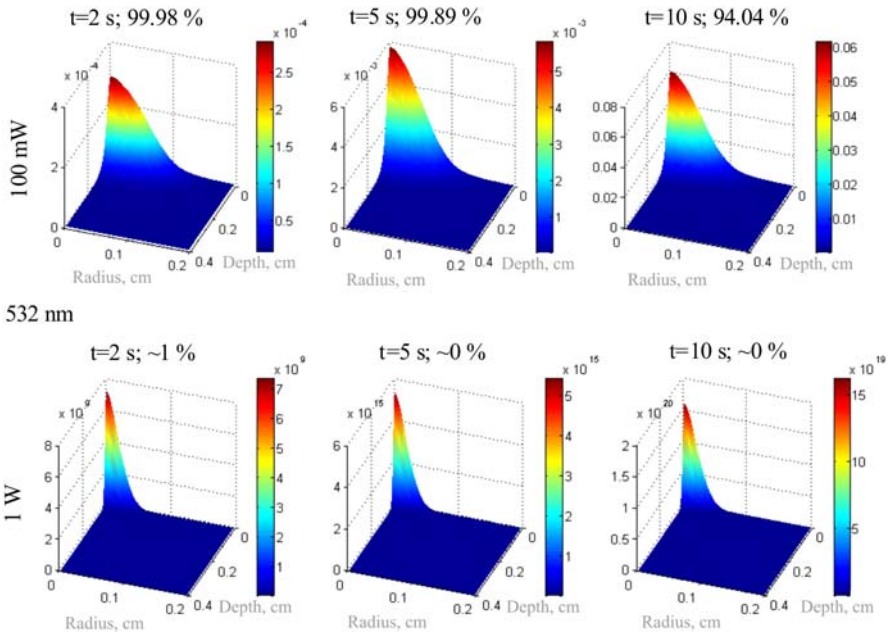

Fig. 7 Thermal damage (colorbar scale) and associated survival fraction of laser irradiated laryngeal skin tissue. The wavelength is 532 nm, and two different powers, 100 mW and 1 W, were used. The irradiances are $3.18\,\mathrm{W}\cdot\mathrm{cm}^{-2}$ and $31.83\,\mathrm{W}\cdot\mathrm{cm}^{-2}$, respectively. The exposition time and survival fraction are noted on each graph

6 Conclusions

In this work, CEM 43 °C and Arrhenius thermal damage models were analyzed and compared when applied to skin optical treatment. The optothermal model used a RTT equation, solved via a Monte Carlo numerical method, for the optical propagation of radiation in tissue. With absorption data from this first analysis, a bio-heat equation, that takes into account conduction, convection, and radiation heat transfer mechanisms, solved via an explicit numerical finite difference method, determined temperature maps in tissue. These maps were used to estimate spatial–temporal thermal damage in the sample, by means of both models. The results showed that the CEM 43 °C model is appropriate when dealing with dosimetry considerations at constant temperature and provides only results compared to those at 43 °C, while the Arrhenius analysis is adequate to predict thermal damage with arbitrary temperature time dependence and gives absolute thermal damage values.

This method allows modeling a general thermotherapy treatment, in such a way that optical source parameters, such as wavelength, power, or exposition duration, can be estimated in order for the treatment to be effective, and for the patient not to suffer from thermal damage in the same tissue or in adjacent ones. The medical praxis related with this kind of therapies, especially on skin diseases due to the accessibility, could be greatly improved by using the Arrhenius integral.

Acknowledgments This work has been carried out partially under the project TEC2006-06548/TCM of the Spanish Ministry of Education and Science. We also thank Dr. Luis Buelta from the Marqués de Valdecilla University Hospital (Santander, Spain), for assistance with the histological structure of skin.

References

1. B.E. Bouma, G.J Tearney, *Handbook of Optical Coherence Tomography* (Marcel Dekker Inc., New York, 2002)
2. T. Vo-Dinh, *Biomedical Photonics Handbook* (CRC Press, Boca Raton, 2003)
3. M.W. Dewhirst, B.L. Viglianti, M. Lora-Michiels, M. Hanson, P.J. Hoopes, Int. J. Hyperth. **19**, 267 (2003)
4. C.F. Bohren, D.R. Huffman, *Absorption and Scattering of Light by Small Particles* (Wiley, New York, 1983)
5. A. Ishimaru, *Wave Propagation and Scattering in Random Media* (IEEE/OUP Series, New York, 1997)
6. G. Yoon, A.J. Welch, M. Motamedi, M.C.J. Van Gemert, IEEE J. Quantum Electron. **23**, 1721 (1987)
7. V.V. Barun, A.P. Ivanov, Int. J. Heat Mass Transf. **46**, 3243 (2003)
8. K.A. Gifford, J.L. Horton, T.A. Wareing, G. Failla, F. Mourtada, Phys. Med. Biol. **51**, 2253 (2006)
9. L. Wang, S.L. Jacques, L. Zheng, Comput. Methods Program Biomed. **47**, 131 (1995)
10. W. Cheong, S.A. Prahl, A.J. Welch, IEEE J. Quantum Electron. **26**, 2166 (1990)
11. F.P. Incropera, D.P. De Witt, *Fundamentals of Heat and Mass Transfer* (Wiley, New York, 1996)
12. H. Arkin, L.X. Xu, K.R. Holmes, IEEE Trans. Biomed. Eng. **41**, 97 (1994)
13. W.J. Minkowycz, E.M. Sparrow, G.E. Schneider, R.H. Pletcher, *Handbook of Numerical Heat Transfer* (Wiley, Inc., New York, 1988)
14. F. Fanjul-Vélez, J.L. Arce-Diego, Lasers Med. Sci. **23**, 168 (2008)
15. J. Ashley, M. Welch, *Optical-Thermal Response of Laser-Irradiated Tissue* (Plenum Press, New York, 1995)